PROCEEDINGS, Thirty-Eighth Workshop on Geothermal Reservoir Engineering
Stanford University, Stanford, California, February 11-13, 2013
SGP-TR-198

A NUMERICAL ANALYSIS ON FLOW IN HYDROTHERMAL SYSTEMS

Larus Thorvaldsson and Halldor Palsson

University of Iceland
Hjardarhaga 2-6
Reykjavik, 101, Iceland
lth31@hi.is, halldorp@hi.is

ABSTRACT

In this paper it is examined how writing specialized codes within the OpenFOAM software framework is applicable to problems involving hydrothermal systems. This is done with two case studies. In the first one, the continuity of mildly compressible flow is stabilized using Fréchet derivatives, enabling the use of very large time steps or treating it as steady state. The second one involves the phase change of water, due to sudden drop in pressure at the top of a water column. The physical properties are determined from the IAPWS-IF97 thermodynamic formulation, which is directly compiled into OpenFOAM. It is also demonstrated how the software framework is able to handle the numerical instabilities that are caused by the discontinuities in physical properties in the phase change region. Both cases demonstrate how the modular nature of the OpenFOAM can be utilized to solve specialized problems involving hydrothermal systems and are validated by analytical solutions.

INTRODUCTION

Numerical simulation of hydrothermal systems has played an important role in the modeling of geothermal reservoirs for the past decades. For researchers it has been used to test competing hypothesis in these complex data-poor environments and in industry numerical simulation has become standard practice in the planning and management of the development of geothermal fields [O'Sullivan, 2001].

The earliest efforts to apply numerical models to geothermal reservoirs were made in the early 1970's, while the usefulness of numerical modelling did not begin to gain acceptance by the geothermal industry until after the 1980 Code Comparison Study [Stanford Geothermal Program, 1980]. Since that study was performed, the experiences gained in carrying out site-specific studies as well as generic reservoir modeling studies have led to a constant improvement in the capabilities of numerical reservoir models.

Numerical modeling of hydrothermal systems is often defined by which components of the system are taken into account. Traditionally they have been divided into hydrological (H), thermal (T), mechanical (M) and chemical (C). Those components are coupled together in a way that is inherently multiscale in nature, such that their temporal and spatial scales vary be several orders of magnitude [Ingebritsen et al., 2010]. Because of the complex nature of those couplings, models involving all four components are rare.

The equations that describe hydrothermal systems are sufficiently complex so that they can only be solved analytically, for a highly idealized set of initial and boundary conditions. Such cases usually only involve one of the four (HTMC) components, where the Theis problem is an example thereof [Theis, 1935]. Some analytical solutions also exists for two components, such as the description of a boiling front moving through a porous medium [Pruess and Celatis, 1987] and the advance of a diffused salt water wedge in a confined aquifer [Henry, 1964]. These analytical solutions are very important in validating numerical models that are supposed to handle more complicated problems.

In order to model realistic hydrothermal systems, numerical models are needed. The current generation of numerical simulators is able to account for multi-phase, multi-component flow. The most versatile are software packages such as Finite Element Heat and Mass Transfer (FEHM) [Keating et al., 2002] and the Transport of Unsaturated Groundwater and Heat (TOUGH) family of codes [Pruess, 1991]. These solvers have been applied to a wide variety of problems, such as CO_2 sequestration, geothermal studies and other environmental issues [Ingebritsen et al., 2010].

Other solvers are more specialized, such as the Complex Systems Modeling Platform (CSMP++)

[Matthäi et al., 2007] and Fully Implicit Seafloor Hydrothermal Event Simulator (FISHES) [Lewis and Lowell, 2009]. They have been developed specifically to allow simulation of high-temperature multiphase flow of NaCl-H_2O fluids. Other codes such as FALCON [Podgorney et al., 2011], developed at Idaho National Labs have focused on the tightly coupled process of fluid-rock interaction.

In this paper the applicability of using a free and open source package named OpenFOAM, in the modeling of hydrothermal systems is examined. OpenFOAM is a highly customizable set of C++ libraries and tools for the solution of problems in continuum mechanics. OpenFOAM is gaining considerable popularity in academic research and among industrial users, both as a research platform and a black-box CFD [Jasak et al., 2007].

The object orientation and operator overloading of C++ has enabled the developers of OpenFOAM to build a framework for computational fluid dynamics that enables modelers to work at a very high level of abstraction [Weller et al., 1998]. This makes it possible to manipulate the set of partial differential equations that describe the problem and customize the solver itself for each class of cases that need to be solved. This will enable researchers with sufficient knowledge about the relevant dynamics of each problem to construct efficient and accurate solvers for it. This is the main motivation for using OpenFOAM, rather than currently existing models.

Since the source code of OpenFOAM is open and freely available, new codes can easily be compiled into the libraries. In this article the IAPWS-IF97 thermodynamic formulation has been implemented in C++ and compiled directly into the code. This allows for considerable improvements in speed and accuracy, where the IAPWS-IF97 is more than five times faster than the older IFC-67 [IAPWS, 2010].

As well as showing how easily an equation of state can be implemented in the previously existing framework, this paper also shows how the underlying equations can be modified in an easy way. This is demonstrated by linearizing the partial differential equations describing the hydrology of the problem using Fréchet derivatives. In this manner it is possible to stabilize the solution for superheated steam, which makes it possible to treat the pressure equation as steady state, allowing for a more computationally efficient solution.

THEORY

Governing equations

For mass conservation the continuity equation must be satisfied

$$\frac{\partial \phi \rho}{\partial t} + \nabla \cdot (\rho \vec{u}) = 0$$

where φ is porosity and ρ is density. In this equation u denotes the superficial velocity, which is a hypothetical velocity calculated as if the fluid were the only thing present in a given cross sectional area. Both phases are also assumed to travel at the same velocity. For pressure-velocity coupling, Darcy's law can be applied

$$\vec{u} = -\frac{\kappa}{\mu}(\nabla p - \rho \vec{g})$$

where κ is permeability, μ is viscosity and g is gravitational acceleration. This gives following equation for groundwater flow

$$\frac{\partial \phi \rho}{\partial t} - \nabla \cdot \left(\frac{\rho \kappa}{\mu} \nabla p \right) + \nabla \cdot \left(\frac{\rho^2 \kappa}{\mu} \vec{g} \right) = 0$$

The energy equation includes both effects from the fluid and the soil, and is given as

$$\begin{aligned} &\frac{\partial}{\partial t}(\phi \rho h + (1-\phi)\rho_s c_s T) + \nabla \cdot (\rho \vec{u} h) \\ =&\nabla \cdot (\Gamma \nabla T) \end{aligned}$$

where ρ_s is the density of soil, c_s is the heat capacity of soil and Γ is the combined conductivity of fluid and soil. If the properties of the soil are assumed to be constant the laplacian of temperature can be broken up in terms of enthalpy and pressure. If the chain rule is also applied to the time derivative of temperature, this equation finally becomes

$$\begin{aligned} &\phi \frac{\partial \rho h}{\partial t} + (1-\phi)\rho_s c_s \left(\frac{\partial T}{\partial h}\frac{\partial h}{\partial t} + \frac{\partial T}{\partial p}\frac{\partial p}{\partial t} \right) \\ &+\nabla \cdot (\rho \vec{u} h) = \nabla \cdot \left(\Gamma \frac{\partial T}{\partial h} \nabla h \right) + \nabla \cdot \left(\Gamma \frac{\partial T}{\partial p} \nabla p \right) \end{aligned}$$

Stabilizing the pressure equation

Since the density is a strong function of pressure in the liquid-vapor phase, it can be accounted for in the time derivative by using a first order Taylor expansion. If it is also assumed that the porosity is not a function of time, the Taylor expansion of the time derivative becomes

$$\frac{\partial \phi \rho}{\partial t} = \phi \frac{\partial \rho}{\partial t} + \phi \frac{\partial}{\partial t} \left. \frac{\partial \rho}{\partial p} \right|_{p=p_0} (p - p_0)$$

The stability of the pressure equation can be increased by linearizing the laplacian term. This is possible by applying a Fréchet derative operator on the term, such that

$$\begin{aligned} \frac{\delta F}{\delta p} &= \frac{\delta}{\delta p} \nabla \cdot \left(\frac{\rho \kappa}{\mu} \nabla p \right) \\ &= \nabla \cdot \left(\frac{\kappa}{\mu} \frac{\partial \rho}{\partial p} \nabla p \right) + \nabla \cdot \left(\frac{\kappa}{\mu} \rho \nabla \right) \end{aligned}$$

this can then be applied to a first order Taylor expansion of the function

$$\begin{aligned} p &= p_0 + \left. \frac{\delta F}{\delta p} \right|_{p=p_0} (p - p_0) \\ &= \nabla \cdot \left(\frac{\kappa}{\mu} \rho \nabla p \right) + (p - p_0) \nabla \cdot \left(\frac{\kappa}{\mu} \frac{\partial \rho}{\partial p} \nabla p_0 \right) \end{aligned}$$

Having applied both the Taylor expansion of the time derivative and the linearization of the laplacian term, the pressure equation becomes

$$\begin{aligned} &\phi \frac{\partial \rho}{\partial t} + \phi \frac{\partial}{\partial t} \left. \frac{\partial \rho}{\partial p} \right|_{p=p_0} (p - p_0) - \nabla \cdot \left(\frac{\kappa}{\mu} \rho \nabla p \right) \\ &- (p - p_0) \nabla \cdot \left(\frac{\kappa}{\mu} \frac{\partial \rho}{\partial p} \nabla p_0 \right) + \nabla \cdot \left(\frac{\rho^2 \kappa}{\mu} \vec{g} \right) = 0 \end{aligned}$$

Analytical solution to the groundwater flow equation

The numerical solution of this problem is then compared to the Theis solution [Theis, 1935], which has the same geometry and governing equations as this problem, but constant physical properties. It is derived from the groundwater equation

$$S \frac{\partial p}{\partial t} = \nabla \cdot (k \nabla p)$$

where *S* is the storativity of the aquifer and *k* is the hydraulic conductivity. These variables can be denoted in terms of the variables that are used in the numerical problem, which gives

$$\phi \frac{\partial \rho}{\partial p} \frac{\partial p}{\partial t} = \nabla \cdot \left(\frac{\kappa}{\mu} \rho \nabla p \right)$$

If the physical properties are approximated to be constant this equation becomes

$$\phi \left. \frac{\partial \rho}{\partial p} \right|_{\rho=\rho_0} \frac{\partial p}{\partial t} = \frac{\kappa}{\mu} \rho_0 \nabla^2 p$$

By applying the similarity transform

$$u = \frac{\phi \mu}{4 \kappa \rho_0 t} \left. \frac{\partial \rho}{\partial p} \right|_{r=r_0} \frac{r^2}{t}$$

a solution for the drawdown, $s = (p_0 - p)/(\rho_0 g)$ can be obtained, such that

$$s = \frac{r_0}{2 \rho_0 g} \left. \frac{\partial p}{\partial r} \right|_{r=r_0} E_1(u)$$

where $E_1(u) = -\mathrm{Ei}(-u)$ and Ei is the exponential integral.

The IAPWS-IF97 thermodynamic formulation

The IFC-67 thermodynamic formulation has now been superseded by the IAPWS-97 formulation. Its current revision consists of a set of equations which cover the following range of validity

$$\begin{aligned} 273.15\mathrm{K} \leq T \leq 1073.15\mathrm{K} \quad &\text{for} \quad p \leq 100\mathrm{MPa} \\ 1073.15\mathrm{K} \leq T \leq 2273.15\mathrm{K} \quad &\text{for} \quad p \leq 50\mathrm{MPa} \end{aligned}$$

where the thermodynamic properties are more accurate than in IFC-67. The algorithm is also more than five times faster than IFC-67 except in the supercritical region where it is approximately three times faster [IAPWS, 2010]

The C++ implementation of IAPWS-IF97 was retrieved from the freesteam project. The primary variables were taken to be pressure and enthalpy, since pressure-temperature formulation has been shown to have more difficulties close to the critical point [Ingebritsen et al., 2010]. Given those two state variables the algorithm returns the steam quality *x*, the density ρ, the temperature *T* and the partial derivatives of all those variables both with respect to pressure and enthalpy. Those values are then used in the system equations, which makes it possible to solve for each time step.

CASE STUDIES

Axisymmetric well

In this case the problem is set up similar to the Theis problem with a one dimensional axisymmetric mesh.

The main difference is that in this case IAPWS-IF97 is used for an equation of state. In this case the fluid is assumed to have a constant enthalpy of 2900 kJ/kg, which for the pressures considered in this case gives superheated steam.

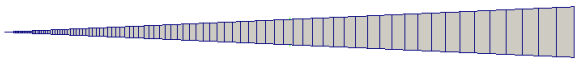

Figure 1: The mesh of the axissymmetric well.

The well is assumed to have a radius of 10cm, and the reservoir is assumed to extend 1 km out from it. In OpenFOAM axisymmetry can be defined by a block, where the two opposing sides normal to the tangential direction are defined with an axisymmetric boundary condition, while the sides normal to the radial direction have the boundary conditions as defined by the problem. The length of the arc in this mesh is set to 5°, while in the radial direction the mesh is divided into 1000 mesh blocks with a cell expansion ratio of 20.

The Neumann boundary condition at the well is assumed to be

$$\left.\frac{\partial p}{\partial r}\right|_{r=r_0} = \frac{Q\mu_0 g}{2\pi r_0 \kappa}$$

where Q is the volume flow rate from the well. At the r_1 = 1km boundary, the pressure is defined as a Dirichlet boundary condition, such that

$$p(r_1) = p_1$$

Two cases are to be considered, one which where the density and viscosity are almost linear, and another one where they are highly non-linear. The linear case is used to validate the numerical solution with the Theis solution, which assumes constant physical properties. This case has the following parameters

$$\begin{aligned} Q &= 5\mathrm{L/s} \\ \mu_0 &= 2.1818 \cdot 10^{-5}\mathrm{Pa \cdot s} \\ \kappa &= 10^{-12}\mathrm{m}^2 \\ p_1 &= 10\mathrm{MPa} \end{aligned}$$

The second case should show the ability of the model to go beyond the Theis solution, with highly non-linear physical properties. In that case they are given as follows

$$\begin{aligned} Q &= 25\mathrm{L/s} \\ \mu_0 &= 1.9293 \cdot 10^{-5}\mathrm{Pa \cdot s} \\ \kappa &= 10^{-12}\mathrm{m}^2 \\ p_1 &= 6\mathrm{MPa} \end{aligned}$$

Phase change

The second case for validation uses both the energy and the pressure equation. The problem is defined as a 10 m high one dimensional water column, with initial enthalpy of 400 kJ/kg. The initial pressure increases hydrostatically in the vertical direction from $8.61 \cdot 10^4$ Pa at the top, but at t = 0 s the pressure is dropped to $7.6 \cdot 10^4$ Pa.

The mesh in this problem is divided evenly into 1000 blocks. In this case both the linearized pressure equation and the energy equation are solved, in a segregated manner.

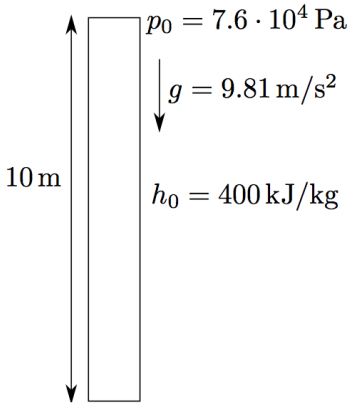

Figure 2: The geometry and the initial conditions of the water column.

RESULTS

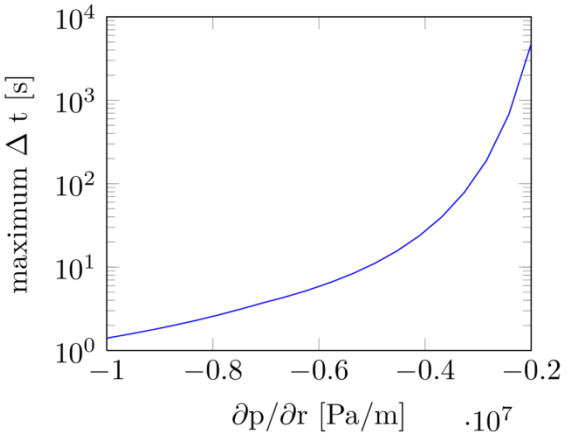

Figure 3: The maximum time step giving a stable solution as a function of the Neumann boundary condition at the well.

Figure 3 shows the maximum time step where the non-linearized equation gives a stable solution, as a

function of the Neumann boundary condition at the well. The figure shows clearly that reaching a stable solution is of course easier with less steep pressure gradient at the well. The stability of the solution seems to increase faster than exponentially as a function of the gradient.

In the case of the linearized pressure equation, it seemed to be unconditionally stable, where a timestep up to 10^{10} was tested.

Comparison of pressure equation to Theis

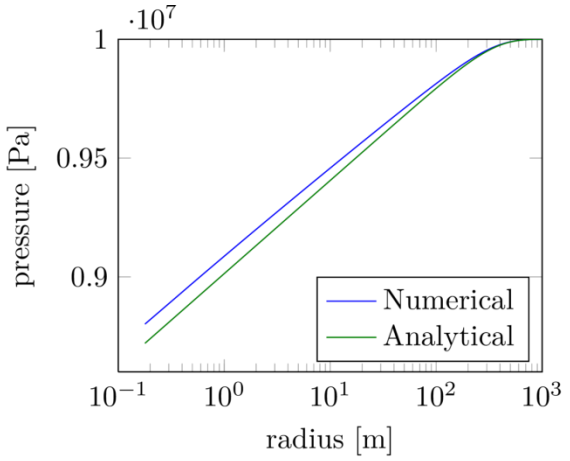

Figure 4: The pressure distribution as a function of distance from the well at time *t* = 3 h.

Figure 4 shows both the numerical and the analytical solution to the axisymmetric well problem, as functions of distance from the well at time t = 3 h. As can be seen from the figure, the two solutions fit very closely.

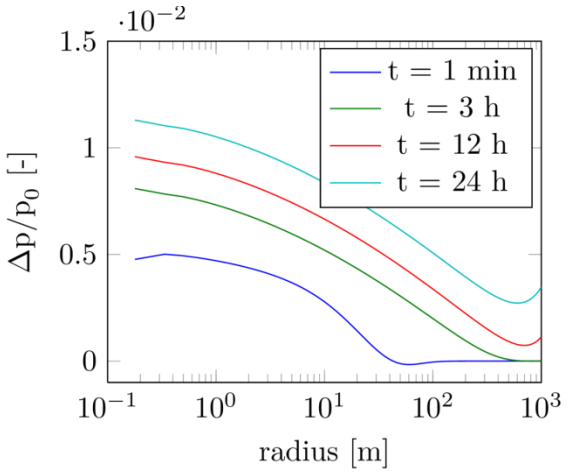

Figure 5: The difference between the numerical and analytical solutions as a function of distance from the well.

Figure 5 shows the difference between the numerical and analytical solution at three different times. The difference increases slightly as time progresses. For the times considered here, the difference seems to be relatively low, through the spatial domain. The difference reaches a maximum where the differences in pressure, and hence the density are highest. Another interesting feature is that after approximately 5 h the change in pressure due to the fluid extraction at the well, reaches the boundary at 1 km distance. Then the error due to the different boundary conditions in the numerical and analytical solution becomes apparent.

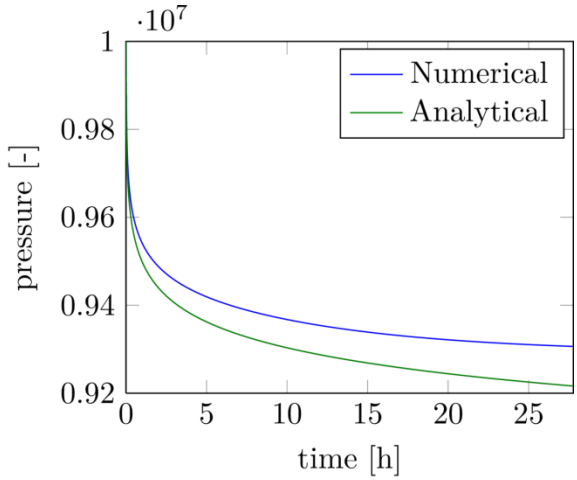

Figure 6: The pressure distribution as a function of time at *r* = 10 m.

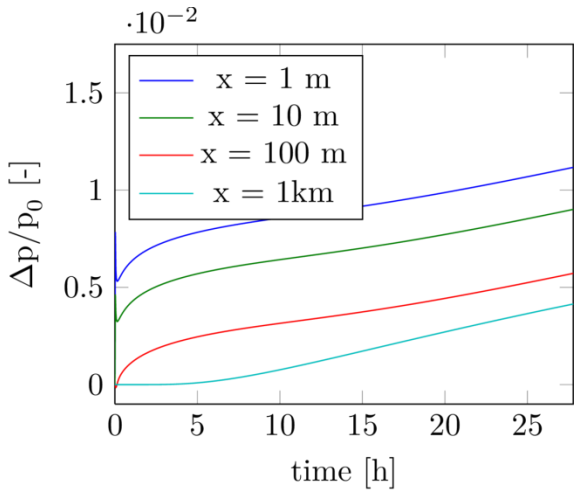

Figure 7: The difference between the numerical and analytical solutions as a function of time.

Figure 6 shows the numerical and analytical solution to the pressure distribution in the axisymmetric problem as functions of time at r = 10 m. Figure 7 shows the difference between the numerical and analytical solutions, scaled with p_0, as a function of time for different distances from the well. From those

figures it can be seen that the difference close to the well increases rapidly in the beginning, and then steadily increases as the two solutions diverge. The error due to the different boundary conditions is most apparent in the r = 1 km line, where the error does not become apparent until after 5 hours.

The main reason for the difference that exists between the numerical and analytical solutions, is that in the numerical solution ρ is a variable inside the laplacian, as can be seen in the pressure equation while a constant ρ_0 is assumed in the analytical solution. If the physical properties are evaluated at the range of pressure that is retrieved from the numerical solution, the maximum relative difference in density is 13.7%. This effect is dominant in generating the difference from the analytical solution, while the viscosity difference of 2.71% and compressibility difference of 0.205% contribute much less to the non-linearity of the problem.

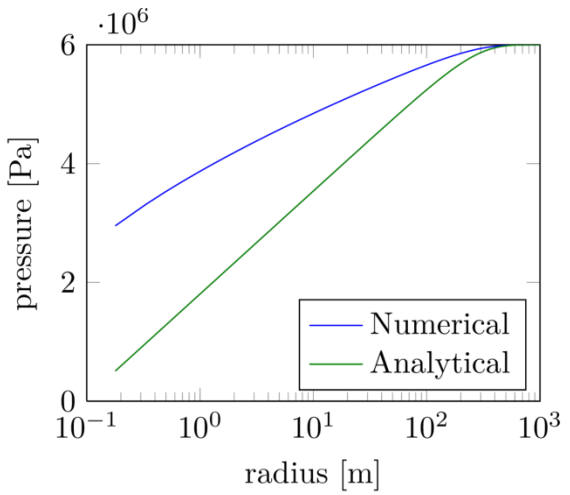

Figure 8: The density as a function of vertical position in the water column at four different times.

Figure 8 shows how the difference between the numerical and analytical solution becomes very large when the boundary conditions are modified to give rise to non-linearity. As can be seen from the figure, the two solutions are very far from each other. If the physical properties are evaluated at the range of pressure that is retrieved from the numerical solution, the maximum relative difference in density is 109 %. This effect is dominant in generating the difference from the analytical solution, while the viscosity difference of 8.94% and compressibility difference of 1.18% contribute much less to the non-linearity of the problem.

Phase change

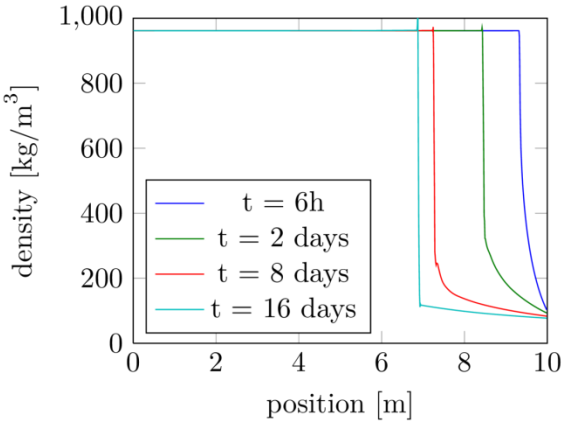

Figure 9: The density as a function of vertical position in the water column at four different times.

Figure 9 shows the density as a function of vertical position in the water column. It is evident that evaporation takes place, very slowly down the water column. This is mainly due to the high permeability and porosity used in the problem. Another interesting feature is how the sudden drop in density seems to become sharper as time progresses. At later times, an overshoot in the density is also evident, which is a result of the discontinuities in physical properties.

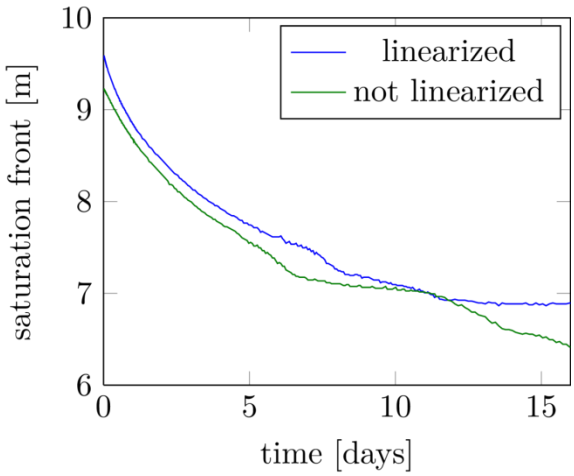

Figure 10: The vertical position of the saturation front as a function of time.

Figure 10 shows the vertical position of the saturation front as a function of time. The front can be seen to progress relatively quickly down the water column in the beginning, and then steadily reaching equilibrium. This effect is perhaps more evident in the linearized case where there are almost no changes to it after day 11.

DISCUSSION

In hydrothermal systems, pressure changes travel much faster than changes in temperature or enthalpy. Therefore it is desirable to treat the pressure equation as steady state, while the energy equation is treated transiently. Having an unconditionally stable solution of the pressure equation is therefore a big advantage in simulating geothermal systems numerically. This makes it possible to conclude that applying Fréchet derivatives can lead to a more stable and computationally efficient solution, at least in the superheated region.

By validating the solver with the Theis solution, it is possible to have some confidence in its solutions. The versatility of the solver has also been displayed by showing its solutions in a region where the equation of state is highly non-linear. This should make it possible to use this solution method of the pressure equation for the hydrological part in future models for hydrothermal systems.

The water column problem shows the ability of OpenFOAM to handle phase change in porous media. An interesting feature there is that the linearized solution is not unconditionally stable. This is probably due to the discontinuities in some physical properties. Because of that small time steps have to be used in that region, in order to arrive at a stable solution despite the linearization of the pressure equation.

CONCLUSION

These are just two examples on how the modular nature of OpenFOAM can be utilized to write specialized codes solving problems involving hydrothermal systems. This makes it possible to simulate some specific dynamics of the system in a computationally efficient way. Being able to manipulate the governing equations of each problem, while still maintaining a very high level of abstraction makes it easier to model phenomena in geothermal systems that are beyond the scope of traditional solvers. These might include fluids in the supercritical region, wellbore-reservoir interaction or near surface behavior.

ACKNOWLEDGEMENTS

The authors would like to thank Eimskip University Fund, Landsvirkjun Energy Research Fund and Geothermal Research Group (GEORG) for their financial support of the project.

REFERENCES

[Henry, 1964] Henry, H. R. (1964). Effects of dispersion on salt encroachment in coastal aquifers. *Sea water in coastal aquifers*, 70.

[Ingebritsen et al., 2010] Ingebritsen, S., Geiger,S., Hurwitz, S., and Driesner, T. (2010). Numericalsimulation of magmatic hydrothermal systems. *Reviews of Geophysics*, (2009):1–33.

[Jasak et al., 2007] Jasak, H., Jemcov, A., andTukovic, Z. (2007). OpenFOAM : A C ++ Libraryfor Complex Physics Simulations ˇ. In*International Workshop on Coupled Methods inNumerical Dynamics*, volume m, pages 1–20.

[Keating et al., 2002] Keating, G. N., Geissman,J. W., and Zyvoloski, G. A. (2002). Multiphasemodeling of contact metamorphic systems and application to transitional geomagnetic ¢ elds. 198:429–448.

[Lewis and Lowell, 2009] Lewis, K. C. and Lowell, R. P. (2009). Numerical modeling of twophase flow in the NaCl-H2O system: Introduction of a numerical method and benchmarking. *Journal of Geophysical Research: Solid Earth*, 114(B5)

[Matthäi et al., 2007] Matthäi, S. K., Geiger, S., Roberts, S. G., Paluszny, A., Belayneh, M., Burri, A., Mezentsev, A., Lu, H., Coumou, D., Driesner, T., and Heinrich, C. A. (2007). Numerical simulation of multi-phase fluid flow in structurally complex reservoirs. *Geological Society, London, Special Publications*, 292(1):405–429.

[O'Sullivan, 2001] O'Sullivan, M. J. (2001). State of the art of geothermal reservoir simulation. *Geothermics*, 30(4):395–429.

[Podgorney et al., 2011] Podgorney, R., Huang, H. C., Lu, C., Gaston, D., Permann, C., Guo, L., and Andrs, D. (2011). FALCON: A Physics Based, Massively Parallel, Fully Coupled, Finite Element Model for Simultaneously Solving Multiphase Fluid Flow, Heat Transport, and Rock Deformation for Geothermal Reservoir Simulation. Technical report, Idaho National Laboratory.

[Pruess, 1991] Pruess, K. (1991). TOUGH2 — A General Purpose Numerical Simulator for Multiphase Fluid and Heat Flow. Technical Report May, Lawrence Berkeley Laboratory, Berkeley, California.

[Pruess and Celatis, 1987] Pruess, K. and Celatis, R. (1987). An analytical solution for heat transfer at a

boiling front moving through a porous medium. 30(12):2595–2602.

[Stanford Geothermal Program, 1980] Stanford Geothermal Program (1980). Proceedings of the Special Panel on Geothermal Model Intercomparison Study. In *Report SGP-TR-42*, Stanford, CA.

[IAPWS (2007). Revised Release on the IAPWS Industrial Formulation 1997 for the Thermodynamic Properties of Water and Steam. Technical Report August 2007, Lucerne, Switzerland.

[Theis, 1935] Theis, C. (1935). The relation between the lowering of the piezometric surface and the rate and duration of discharge of a well using groundwater storage. *Transactions – American Geophysical Union*, 16:519–524.

[Weller et al., 1998] Weller, H. G., Tabor, G., Jasak, H., and Fureby, C. (1998). A tensorial approach to computational continuum mechanics using object-oriented techniques. *Computers in Physics*, 12(6).